

Received 6 May 2025, accepted 21 May 2025, date of publication 28 May 2025, date of current version 5 June 2025.

Digital Object Identifier 10.1109/ACCESS.2025.3574340

RESEARCH ARTICLE

Impact of Multiple CPU Cores to the Forensic Insights Acquisition From Mobile Devices Using Electromagnetic Side-Channel Analysis

LOJENAA NAVANESAN^{1,2}, (Member, IEEE), KASUN DE ZOYSA², (Member, IEEE),
AND ASANKA P. SAYAKKARA², (Senior Member, IEEE)

¹Department of ICT, University of Vavuniya, Vavuniya 43000, Sri Lanka

²University of Colombo School of Computing, Colombo 00700, Sri Lanka

Corresponding author: Asanka P. Sayakkara (asa@ucsc.cmb.ac.lk)

ABSTRACT Modern processors tend to incorporate multiple CPU cores. These multiple CPU cores, running at the same or different clock frequencies, enable the effective distribution of workload and efficiency in energy consumption. Although Electromagnetic Side-Channel Analysis (EM-SCA) has been shown to be an effective and non-invasive method to acquire forensic insights from smartphones and Internet of Things (IoT) devices, the presence of multiple CPU cores has the potential to cause disruptions in this process. This research focuses on analysing the impact of multi-core CPU emissions — specifically the iPhone 13 and iPhone 14 Pro — on the EM-SCA-based forensic insights acquisition procedure. To achieve this, we developed a novel multi-core EM-SCA model specifically for iPhone models by integrating electromagnetic (EM) radiation traces captured from different core clusters of a single device. The developed multi-core model is then subjected to three transfer learning processes: inductive learning, feature extraction, and fine-tuning. The model is tested using individual single-core datasets collected at specific system-clock frequencies of the device. The findings of both smartphones indicate that inductive transfer learning consistently yields poor results, ranging between 5% and 20%, regardless of the core cluster. Although feature extraction provides moderate accuracy for certain datasets — around 50% to 70% for the iPhone 13 and 20% to 92% for the iPhone 14 Pro — it is the fine-tuning process that proves to be the most effective. Fine-tuning supports a wide range of datasets across different system-clock frequencies, achieving classification accuracy as high as 99%. This highlights fine-tuning as the most reliable transfer learning technique for multi-core forensic investigations. We also tested for catastrophic forgetting to evaluate the robustness of the multi-core model when using single-core datasets from the same devices. The results demonstrate that the accuracy of the multi-core model remains unchanged, even after the transfer learning process across various datasets.

INDEX TERMS Catastrophic forgetting, cross-device portability, digital forensic investigation, EM-SCA model, multi-core devices.

I. INTRODUCTION

Digital Forensics is a specialised field that is focused on the recovery, analysis, and preservation of digital evidence from electronic devices. It plays a crucial role in investigations involving cybercrimes, data breaches, and other legal matters

The associate editor coordinating the review of this manuscript and approving it for publication was Wei Xu¹.

where digital evidence is pivotal [1], [2]. Digital forensics experts use various tools and techniques to extract data, including deleted files, encrypted information, and logs, while ensuring the integrity of the evidence for use in legal proceedings [3], [4]. This discipline is essential to ensure the smooth execution of legal and corporate investigations to uncover criminal and other misconduct in an increasingly technology-driven world.

In the current era, most forensic investigations heavily rely on smart devices. This is due to the fact that smart devices are increasingly present in everyday environments in contrast to desktop and laptop computers. There is a continuous influx of new smart devices, each with considerable modifications and advances in technology [5], [6], [7]. These devices — ranging from smartphones and tablets to smartwatches and IoT devices — store vast amounts of data that can be crucial to unravelling the details of a crime. However, this rapid evolution of smart device technology poses a significant challenge to forensic experts [8], [9]. The diversity in hardware and software configurations, coupled with the increased use of encryption and other security measures, makes it difficult to effectively access, analyse, and interpret data from smart devices. As a result, digital forensic researchers are increasingly turning to advanced techniques, such as Electromagnetic Side-Channel Analysis (EM-SCA) to retrieve insight from these devices without necessarily having to physically tamper with them [10], [11].

EM-SCA leverages the unintentional electromagnetic (EM) radiation emission of electronic devices to infer sensitive information, such as encryption keys, user activity, or stored data [12], [13]. The EM-SCA technique has been established as a powerful method to identify internal software behaviours of dedicated smart devices, including smartphones, IoT devices, smart wearables, and more. Although this technique has proven effective in revealing forensic insights from such devices, EM-SCA-based machine learning (ML) models are typically tailored to specific processor types, as they are trained on the EM data of those processors [14], [15]. As a result, these models lack cross-device portability, limiting their broader forensic application. To address this challenge, Navanesan et al. proposed enhancing the portability of EM-SCA-based ML models to enable more versatile acquisition of forensic insight across different types of smart devices [16].

Cross-device portability refers to the reuse of EM-SCA-based ML models across different devices. When applying a trained EM-SCA-based ML model from one device to another, initial tests often yield poor results. Therefore, transfer learning is required to enhance cross-device portability of these models [16]. In previous work, it has been hypothesised that several factors contribute to these poor results, including external environmental EM noise, manual handling during the data capture process, and the emergence of multi-core smart devices. In this study, we aimed to analyse the cross-device portability of multi-core devices to ensure effective forensic insight acquisition. To achieve this, we selected devices from a single manufacturer with a multi-core architecture—specifically, the iPhone 13 and iPhone 14 Pro. The key contributions of this research are as follows:

- **Cross-Device Portability Analysis of Multi-core Devices:**

We analysed the iPhone 13 and iPhone 14 Pro from the perspective of multi-core devices to ensure cross-device portability for forensic insight acquisition.

- **Validation of Catastrophic Forgetting:**

We validated the phenomenon of catastrophic forgetting in the EM-SCA-based ML model, which is crucial for maintaining the performance of the model when applying transfer learning techniques.

This study provides valuable insights into the challenges and opportunities of utilising multi-core devices for digital forensic investigations. Evaluating the performance of EM-SCA in extracting forensic insights from multi-core smart devices not only helps to understand the capabilities and limitations of EM-SCA as a forensic tool, but it also helps to develop best practices and protocols for its use in real-world investigations. As technology advances, forensic experts must continuously adapt their techniques and methodologies to keep up with the evolving landscape of digital evidence.

This study focuses exclusively on analysing multi-core devices using a single type of smartphone—the iPhone 13 and iPhone 14 Pro—as a case study, which were selected for their representativeness of current high-end mobile devices. Although these models provide valuable insights into the performance and software behaviour of modern smartphones, it is important to note that the results may vary with different smartphone brands, operating systems, or hardware configurations. Although this represents a limitation, as the analysis is limited for a manufacturer, it serves as a stepping stone towards broader research. Future studies incorporating a wider range of devices could further enrich the understanding of these dynamics across diverse mobile platforms. By establishing a framework for cross-device portability and validating our findings on these devices, we aim to provide a pathway for future analyses of multi-core devices from different manufacturers. This limitation underscores the need for additional studies to generalise the results across a wider range of device architectures and brands. This approach allows us to provide insights into cross-device portability while laying the groundwork for future research on devices from diverse manufacturers.

The rest of the paper is organised as follows. Section II provides an overview of the foundational concepts related to EM-SCA, forensic insight acquisition, and multi-core devices, along with a discussion of state-of-the-art techniques and advancements in these domains. Section III outlines the experimental methodology for developing the EM-SCA-based ML model, with a specific focus on multi-core mobile devices, particularly the iPhone 13 and iPhone 14 Pro. Section IV presents the experimental results on applying various transfer learning techniques for cross-device portability in multi-core mobile devices and evaluates catastrophic forgetting to assess the robustness of the multi-core EM-SCA-based ML model. Section V provides a detailed discussion of the methodology and the results, highlighting key findings, underlying reasons, and potential limitations. Finally, Section VI offers a brief summary of the findings and suggests future research directions.

II. FORENSIC INSIGHT FROM MULTI-CORE DEVICES

A. EM-SCA FOR FORENSIC INSIGHT ACQUISITION

Electronic devices unintentionally leak information about their internal operations through various channels, such as power consumption, acoustic emissions, heat, EM radiation, timing variations. These channels are collectively known as side-channels [18], [19], [20]. Multiple side-channel analysis techniques are available, including Correlation Electromagnetic Analysis (CEMA), Differential Electromagnetic Analysis (DEMA), Correlation Power Analysis (CPA), TEMPEST attacks, and Simple Power Analysis (SPA) [13], [21], [22], [23]. In recent years, cutting-edge innovations have integrated machine learning and deep learning algorithms [24], [25], [26], [27], [28], where models such as Convolutional Neural Networks (CNNs) [29], [30], Recurrent Neural Networks (RNNs) [31], LSTM [32], and Transformer-based architectures automatically identify subtle features in leaked signals [33], [34]. In addition to these, the emerging literature has begun to incorporate spectral analysis, wavelet transform techniques, and sparse signal recovery to enhance feature extraction from noisy datasets [35]. These advanced techniques not only refine the analysis of complex side-channel signals but also facilitate real-time forensic investigations by reducing computational overhead.

Smart devices pose significant challenges for forensic investigators due to their inherent characteristics, such as encrypted data, customised and personalised configurations, rapidly evolving technologies, and real-time data processing [36], [37]. These factors often necessitate physical tampering of the devices to carry out an investigation. However, such actions have the potential to make acquired evidence inadmissible in courts and violate law enforcement protocols related to the handling of evidence [38], [39]. Therefore, non-invasive techniques are more appropriate for investigating smart devices.

To address these challenges, Sayakkara et al. proposed the application of EM-SCA as a non-invasive forensic insight acquisition method. They demonstrated that it is possible to identify EM radiation patterns corresponding to the internal software behaviour of specific smartphones and IoT devices. Although the insights gained through EM-SCA may not always be admissible as direct evidence in courts of law, they can significantly aid investigators by providing valuable forensic leads [10], [11], [15].

B. CROSS-DEVICE PORTABILITY OF EM-SCA

Although the EM-SCA-based forensic insight acquisition procedure was developed to acquire forensic insight from smart devices, questions remain about its applicability across a variety of devices with different or similar processors. The proposed procedure uses specifically trained ML models for individual processor types, raising concerns about its generalisability. In the context of digital forensic investigations, this lack of generalisation could pose challenges for

forensic investigators who need to analyse different types of devices. Without a generalised EM-SCA-based ML model, investigators would need to retrain an EM-SCA-based ML model from scratch for each new device type, which is time-consuming and inefficient [14].

To address this issue, Navanesan et al. introduced the concept of cross-device portability and explored a potential approach to ensure it. Their approach aims to ensure that the EM-SCA-based ML model can be generalised and effectively applied to a wide range of devices, even those with varying processor types. Thus, cross-device portability has the potential to significantly enhance the utility of EM-SCA-based forensic insight acquisition in forensic investigations, allowing investigators to apply a trained model across different devices without the need for extensive retraining [16], [17].

In addition to EM-SCA cross-device portability, Yu et al. present an innovative approach to enhancing the quality of side-channel traces by reducing noise through an unsupervised deep learning framework. The proposed method is designed to work on different devices, such as different ARM and APR-based microprocessors, addressing the challenge posed by variability in noise patterns inherent in cross-device analysis. By leveraging unsupervised learning techniques, the framework effectively transforms noisy side-channel signals into cleaner, more informative traces without the need for labelled training data [40].

C. MULTI-CORE SMART DEVICES FOR FORENSIC INVESTIGATION

By integrating multiple CPU cores within a single device, smart devices can handle complex tasks simultaneously, providing faster and more efficient processing power [41], [42]. This architecture is particularly beneficial for running resource-intensive applications, such as those involving artificial intelligence, real-time data processing, and gaming. In addition, multi-core processors improve energy efficiency by distributing workloads across multiple cores, reducing the need for high power consumption in a single core [43]. As the demand for more sophisticated and responsive smart devices grows, multi-core architectures continue to play a pivotal role in meeting these needs in smartphones, tablets, IoT devices, and wearables [44].

Furthermore, Sayakkara et al. discussed modern battery-powered devices that use energy-saving techniques such as dynamic voltage-frequency scaling (DVFS) and multi-core clustering (for example, ARM's big.LITTLE) that adjust CPU clock frequencies based on workload to optimise energy efficiency and performance. However, these frequency adjustments can obscure key signals used in EM-SCA attacks, highlighting the need for future research to address these challenges [14]. Moreover, while Sayakkara et al. and Navanesan et al. conducted extensive analyses on smartphones and IoT devices featuring multi-core architectures, their work did not delve into the EM traces generated

by individual CPU cores. This omission leaves unexplored potential variations in core-specific EM emissions, which highlights a crucial area for future research in EM-SCA-based forensic investigations [14], [16], [17].

In the context of digital forensics, understanding the influence of multi-core architecture on retrieving internal software behaviours through EM-SCA from smart devices is essential. Multi-core processors, which are common in modern smart devices, can complicate the process of analysing and acquiring EM-based forensic insights. Specifically, it is crucial to examine how the system clock frequency of individual cores affects the overall EM radiation pattern of the device. This involves determining the extent to which the system clock frequency of a specific core contributes to the identification of that core during the EM-SCA-based forensic insight acquisition procedure.

To effectively implement EM-SCA-based ML models across different devices, especially in the context of cross-device portability, it is important to verify the role of multi-core architectures and their associated system clock frequencies. This verification process helps ensure that the model can accurately identify the software activities of specific cores within a multi-core system. By understanding these dynamics, investigators can better assess the performance of the EM-SCA-based ML model and its ability to acquire forensic insights from a wide range of devices, regardless of their processor configurations.

III. METHODOLOGY

A. EM-SCA MODEL OF MULTI-CORE DEVICES

This section provides a detailed overview of the experimental procedure, including the steps for collecting EM radiation from the selected multi-core devices and evaluating its performance at various system clock frequencies of each core. The evaluation is carried out by developing the EM-SCA-based ML models to analyse captured EM data from target devices. The next section covers the verification of cross-device portability across various datasets derived from each frequency, followed by a section that evaluates catastrophic forgetting in the cross-device portability of the EM-SCA model.

1) DATA COLLECTION FROM MULTI-CORE DEVICES

This study commenced with the selection of target devices featuring multi-core architectures. For our experiment, we chose the iPhone 13 and iPhone 14 Pro. This choice was influenced by earlier research by Navanesan et al. [16], who examined cross-device portability across various iPhone models. Their findings provide a valuable foundation for evaluating the performance and results specific to multi-core devices in this study. Table 1 provides detailed specifications, including the system clock frequencies for each core cluster of the selected iPhones.

For the first time, we have planned an innovative approach to collecting EM traces from multi-core devices by

employing multiple *HackRF One* Software Defined Radio (SDR) devices [45]. This method aims to enhance the accuracy and efficiency of EM trace acquisition, particularly from complex multi-core architectures. Our experiment involves two different iPhone models, each with distinct system clock frequencies corresponding to various clusters of cores, as detailed in Table 1. By leveraging multiple SDRs, we can simultaneously monitor and record the EM emissions of these diverse cores, providing a comprehensive dataset for analysis. Figure 1 illustrates the steps of the data collection procedure.



FIGURE 1. Steps of EM data collection from the multi-core device.

Multiple SDR Configuration involves utilising two HackRF One SDR devices, each configured to target specific frequencies associated with the core clusters of the respective iPhone devices. This configuration allows for parallel data collection, reducing the time required and increasing the resolution of captured EM traces. Frequency tuning involves each SDR being precisely tuned to the system clock frequency of the target core cluster, ensuring optimal signal acquisition and minimising interference. Figure 2 illustrates the proposed data collection setup utilising two HackRF One SDR devices. The diagram shows the arrangement of equipment, connection interfaces, and the flow of data from iPhones to the data processing system.

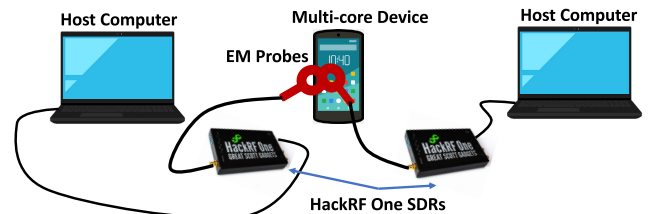


FIGURE 2. Schematic representation of the experimental setup for EM trace collection using multiple HackRF One SDRs.

EM data were acquired while the device was performing 10 distinct software activities with corresponding labels: *calendar-app*, *camera-photo*, *camera-video*, *email-app*, *gallery-app*, *home-screen*, *idle*, *phone-app*, *sms-app*, and *web-browser-app*. When a user opens one application while closing others on a smartphone, the operating system dynamically manages the remaining background applications to optimise performance and resource utilisation. Modern mobile operating systems, such as Android and iOS, typically suspend or partially terminate non-active applications to free up memory and processing power for the foreground application [46], [47]. Nevertheless, certain essential applications, such as music players, navigation tools, and messaging services, may continue to operate in a limited capacity to ensure uninterrupted functionality [48]. This strategic resource management not only enhances the responsiveness

TABLE 1. Specifications of the iPhone devices used in the experiment, including details of their SoCs, architectures, and system clock frequencies for each core cluster.

| Device Name | System-on-Chip | Architecture | System-clock frequency-1 (f_1) | System-clock frequency-2 (f_2) |
|---------------|------------------|--------------|------------------------------------|------------------------------------|
| iPhone 13 | Apple A15 Bionic | ARMv 8.5-A | 3.23 GHz (2 cores) | 1.82 GHz (4 cores) |
| iPhone 14 Pro | Apple A16 Bionic | ARMv 8.6-A | 3.46 GHz (2 cores) | 2.02 GHz (4 cores) |

of the active application but also contributes to improved battery life and overall system performance [46], [48].

In our experimental setup, EM data acquisition was performed while executing a specific application on the smartphone. Prior to launching the chosen application, we manually terminated all other background applications to ensure that the EM signals obtained were solely related to the activity of the selected *app*. This approach helped to minimise any interference from background processes, allowing for more accurate data collection during the analysis. The data acquisition process is outlined as follows:

- **Data Collection from iPhone 13**

Two SDR devices were utilised to capture EM traces: one tuned to 3.23 GHz and the other to 1.82 GHz, targeting the iPhone 13.

- **Data Collection from iPhone 14 Pro**

Two SDR devices were configured for EM data acquisition: one tuned to 3.46 GHz and the other to 2.02 GHz, with the iPhone 14 Pro serving as the target device.

2) DATA ACQUISITION PROCESS

The data acquisition process begins by identifying the target device and its corresponding software activities, followed by recording the EM radiation emitted during execution. The system clock frequency is adjusted on the host computer using GNU Radio Companion (GRC) for precise tuning. The experiment employs the HackRF One SDR, operating within a frequency range of 1 MHz to 6 GHz and a maximum sampling rate of 20 MHz [14]. The GNU Radio library and GRC facilitate the configuration and data processing, forming the EM data processing pipeline. To enhance signal reception, the RF Explorer near-field H-loop antenna is connected to the HackRF One for close-proximity data acquisition from the target device. The optimal signal reception point is manually determined by moving the near-field antenna while plotting the spectrogram at the CPU clock frequency of the DUT. Once the strongest signal is identified, it is fixed for EM trace acquisition. While prior research has explored automated tools for optimising signal reception [49], this study relies on manual observation to determine the ideal acquisition position for each target device. The existing EM capture process is illustrated in Figure 3.

In this experiment, two HackRF One SDRs are utilised to capture EM radiation at different system-clock frequencies based on the core clusters of the target device. Each SDR is connected to a dedicated host computer, and each system runs its own instance of the GRC application. Figure 4 provides an illustration of the experimental setup, showcasing

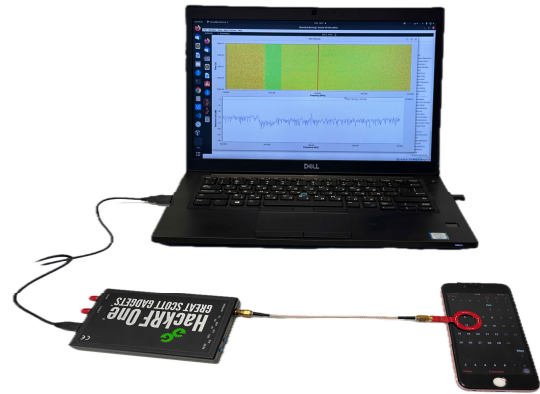


FIGURE 3. The actual EM capture setup consists of an H-loop near-field antenna connected to a HackRF One SDR, which interfaces with a computer running GNU Radio Companion for signal processing.

the target device and the dual SDR configuration used for EM data acquisition. Since our target devices are well-known commercial brands, their SoC locations are publicly documented. This familiarity allows us to accurately map the SoC position and strategically place the H-loop near-field antenna directly above it, ensuring optimal EM signal acquisition.



FIGURE 4. The actual setup for acquiring EM data from multi-core target devices using multiple HackRF One SDRs.

As illustrated in Figure 4, two HackRF One SDR devices simultaneously capture EM radiation using individual H-loop near-field antennas connected to each SDR, operating at a high sampling rate of 20 MHz. During the data collection process, a selected software activity runs on the target device. For example, consider an iPhone 14 Pro executing the *web_browser-app*. At the same time, the two HackRF One SDR devices are tuned to 3.46 GHz and 2.02 GHz using their respective GRC flow graphs, as shown in Figures 5 and 6. These frequencies correspond to the two core clusters of the Apple A16 Bionic processor, each operating at a different system-clock frequency. EM traces captured concurrently by both SDR devices for the same duration of time are stored as *.cfile* files (e.g., *web_browser-app.cfile*) on their respective host computers. This process is repeated for other software activities at both frequencies to ensure comprehensive data collection.

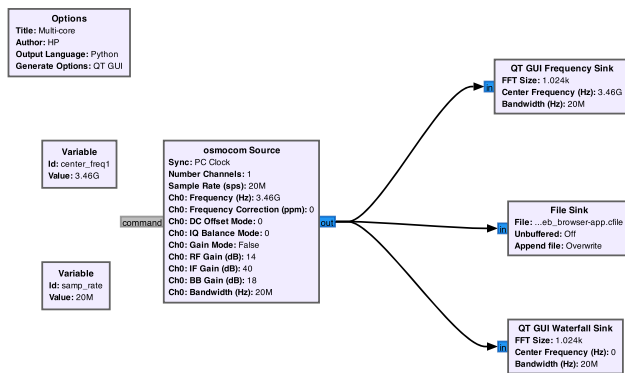


FIGURE 5. Flow graph of the iPhone 14 Pro tuned to a higher system-clock frequency of 3.46 GHz.

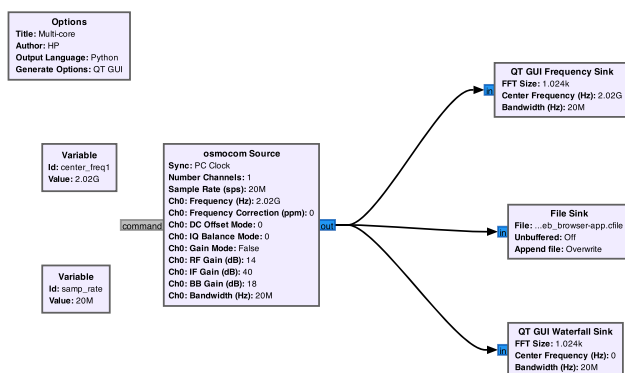


FIGURE 6. Flow graph of the iPhone 14 Pro tuned to a lower system-clock frequency of 2.02 GHz.

The GRC software utilises a flow graph to configure parameters for data acquisition. In this setup, the sample rate defines the number of samples per second, while the system-clock frequency of each core of the iPhone is assigned to the variable *centre frequency*. The *Osmocom Source* block represents the attributes of the HackRF One device, while the *Frequency Sink* block and the *Waterfall Sink* block are used to identify peak signals and analyse the EM signal patterns at the designated frequency. Additionally, the *File Sink* block is employed to store the acquired EM traces in the *.cfile* format. The amplification settings were determined through empirical experimentation, testing various configurations to optimise signal clarity across different devices, as explored in previous research. Based on the findings from this study, the radio frequency power amplifier (RF), low-noise amplifier (IF), and variable-gain amplifier (BB) were consistently set to 14 dB, 40 dB, and 18 dB, respectively, throughout the experiments to ensure reliable signal acquisition [14], [17]. Furthermore, for the iPhone 13, the centre frequencies in both GRC flow graphs were set to 3.23 GHz and 1.82 GHz, respectively.

3) DATA PREPARATION FOR EM-SCA MODEL

To use EM trace data with ML algorithms, it needs to be pre-processed to extract relevant features. When a target

device emits EM radiation, it reveals information about its internal behaviour through various EM frequencies close to the system clock frequencies of the CPU cores. Although we account for the system clock frequency of multiple cores, external noise can obscure these important signal variations in the time domain. Converting the time-domain signal to the frequency domain with techniques such as Short-Time Fourier Transform (STFT) enhances the individual frequency components, making it easier to identify and extract valuable information.

The time-domain EM trace files were processed using STFT with a window size of 2048 in-phase/quadrature (I/Q) samples and an overlap of 256 I/Q samples, resulting in a 12% overlap for each STFT window. A window size of 2048 I/Q samples and an overlap of 256 I/Q samples were selected based on empirical testing, evaluating various configurations against the classification accuracy they produced. Through systematic experimentation, this particular setting demonstrated the best balance between preserving important signal features and ensuring computational efficiency. Additionally, existing studies [15] have also recommended using a window size of 2048 and an overlap of 256 for similar types of EM side-channel analysis, further supporting our choice. This process generates a two-dimensional dataset: The frequency dimension has 2048 columns (i.e., frequency channels), and the time dimension consists of time points, each representing a set of 2048 samples from the original time-domain signal. Each STFT dataset is labelled according to the original software activity of the smart device, which serves as a class for the ML algorithm. The frequency dimension of each STFT dataset, which contains 2048 features, is used as the feature vector for the ML algorithm.

4) COMBINED DATASET FOR THE MULTI-CORE EM-SCA MODEL

After collecting EM data from the target device at both system-clock frequencies, the two sets of EM traces are merged to develop an EM-SCA-based ML model. This integration results in a combined model, referred to as the *multi-core model* for the iPhone 13 and iPhone 14 Pro, which incorporates EM emissions from both core frequencies. Utilising dedicated SDRs for each core cluster enhances the quality of captured EM traces, enabling the detection of subtle variations that can reveal underlying computational processes or potential security vulnerabilities.

For each specific software activity on the target device, two distinct EM traces were recorded, corresponding to the different system-clock frequencies. In total, data were collected for ten different software activities, each executed sequentially while two separate SDR devices captured EM traces simultaneously. Consequently, each software activity produced two independent sets of EM traces, which were recorded by individual SDRs.

To prepare the dataset for training a deep neural network, these EM traces were merged, aligning multiple feature inputs under each software activity. For model training,

10,000 STFT windows were extracted per class at each frequency, resulting in 20,000 instances per class when combining both frequencies. With a total of ten software activity classes, this approach generated a dataset comprising 200,000 training instances.

5) MACHINE LEARNING APPROACHES FOR EM-SCA DATA ANALYSIS

The dataset enables advanced analysis techniques, such as assessing side-channel attacks and profiling performance. An MLP neural network was trained separately for each device to classify its software behaviour using EM trace files. In other words, two distinct MLP models were trained independently on EM traces collected from iPhone 13 and iPhone 14 Pro. Table 2 illustrates the MLP network architecture, which includes an input layer with 2048 features and an output layer with nodes corresponding to the number of classes for each device. The network features five hidden layers with ReLU activation and an output layer with Softmax activation. For training, 20,000 samples per class (10,000 samples per core's system-clock frequency) were used, with the data split into 90% for training and 10% for testing. Given the large volume of data, a 10% test set remains substantial for evaluation. While an 80:20 split is a common practice, we opted for a 90:10 split to maximise the training data available for model learning, which is particularly beneficial when working with a limited dataset. This larger training set allows the model to capture underlying patterns more effectively, while the 10% test set provides a reliable performance assessment. Furthermore, our approach is validated through k-fold cross-validation on the combined dataset. Each model was trained for 30 epochs with the network using stochastic gradient descent (SGD) as the cost/optimisation function with a learning rate of 0.001 and sparse categorical cross-entropy as the loss function, and a validation dataset consisting of 10% of the training data was randomly selected for each epoch. The Keras API from the TensorFlow library was used for developing and testing the networks.

TABLE 2. The structure of the deep neural network architecture for the combined dataset from multi-core device with data from 10 different internal software behaviours.

| Layer Type | Output Shape | No. of Parameters |
|----------------------------|--------------|-------------------|
| dense (Dense) (ReLU) | (None, 1400) | 2,868,600 |
| dense_1 (Dense) (ReLU) | (None, 800) | 1,120,800 |
| dense_2 (Dense) (ReLU) | (None, 500) | 400,500 |
| dense_3 (Dense) (ReLU) | (None, 200) | 100,200 |
| dense_4 (Dense) (ReLU) | (None, 100) | 20,100 |
| dense_5 (Dense) (Softmax) | (None, 10) | 1,010 |
| Total trainable parameters | | 4,511,210 |

B. CROSS-DEVICE PORTABILITY OF THE MULTI-CORE DEVICE

An EM-SCA-based ML model is created using the combined dataset of each CPU core's EM emissions collected from the

target devices, iPhone 13 and iPhone 14 Pro, named the multi-core model. The cross-device portability of the multi-core model is tested in two ways: first, using the single-core dataset (collected from one frequency) used to build the multi-core model. Second, using various datasets collected at the specific frequencies of the core clusters at different times. This evaluation aims to verify the robustness and applicability of the multi-core model across datasets captured at different times but at varying core-cluster frequencies.

1) ASSESSING INDIVIDUAL CORE DATASETS COLLECTED AT DIFFERENT TIME INTERVALS

Subsequently, multiple EM traces were collected at various system-clock frequencies of the cores in the dedicated device both at the same and different times to evaluate the cross-device portability of the combined model. This includes datasets from all core frequencies of the specific target device, as explained in Section III-A4. Identical iPhone 13 and iPhone 14 Pro devices were used to collect multiple datasets at various core frequencies over different time intervals. The dataset names and their corresponding details are presented in Table 3.

TABLE 3. Index of datasets and their corresponding details for the multi-core target devices.

| Dataset Index | Device Name | System-clock-frequency (GHz) | Time interval |
|--------------------------|---------------|------------------------------|---------------|
| i13-I- f_1 - t_1 | iPhone 13_I | 3.23 (f_1) | t_1 |
| i13-II- f_1 - t_2 | iPhone 13_II | 3.23 (f_1) | t_2 |
| i13-III- f_1 - t_3 | iPhone 13_III | 3.23 (f_1) | t_3 |
| i13-IV- f_1 - t_4 | iPhone 13_IV | 3.23 (f_1) | t_4 |
| i13-IV- f_2 - t_4 | iPhone 13_IV | 1.82 (f_2) | t_4 |
| i13-IV- f_1 - t_5 | iPhone 13_IV | 3.23 (f_1) | t_5 |
| i13-IV- f_2 - t_6 | iPhone 13_IV | 1.82 (f_2) | t_6 |
| i14Pro- f_1 - t_7 | iPhone 14 pro | 3.46 (f_1) | t_7 |
| i14Pro- f_2 - t_7 | iPhone 14 pro | 2.02 (f_2) | t_7 |
| i14Pro- f_1 - t_8 | iPhone 14 pro | 3.46 (f_1) | t_8 |
| i14Pro- f_1 - t_9 | iPhone 14 pro | 3.46 (f_1) | t_9 |
| i14Pro- f_1 - t_{10} | iPhone 14 pro | 3.46 (f_1) | t_{10} |
| i14Pro- f_1 - t_{11} | iPhone 14 pro | 3.46 (f_1) | t_{11} |
| i14Pro- f_2 - t_{12} | iPhone 14 pro | 2.02 (f_2) | t_{12} |
| i14Pro- f_2 - t_{13} | iPhone 14 pro | 2.02 (f_2) | t_{13} |
| i14Pro- f_2 - t_{14} | iPhone 14 pro | 2.02 (f_2) | t_{14} |
| i14Pro- f_2 - t_{15} | iPhone 14 pro | 2.02 (f_2) | t_{15} |

C. CATASTROPHIC FORGETTING

Catastrophic forgetting, also known as catastrophic interference, is a phenomenon in neural networks where a model loses previously learnt information when learning new data [50], [51]. This issue is particularly common in sequential learning scenarios, such as transfer learning or when training on multiple tasks. When a model is trained on a new task, the updates to the network's weights can overwrite the knowledge gained from previous tasks, leading to a significant drop in performance on earlier tasks. This challenge is a major concern in the development of artificial intelligence (AI) systems that need to retain knowledge over time and across different domains, necessitating strategies such as

regularisation techniques, rehearsal methods, or architectural changes to mitigate its effects [52].

The EM-SCA-based ML models are fundamentally constructed using MLP neural networks. To ensure the generalisability of the model across various devices, the cross-device portability of the EM-SCA model incorporates transfer learning. However, it is crucial to assess the potential for catastrophic forgetting within the EM-SCA-based ML models when applying transfer learning between different devices. This assessment is essential to maintain the integrity and effectiveness of the model, as catastrophic forgetting could lead to the loss of previously learnt knowledge when adapting the model to new devices.

To ensure the integrity of the EM-SCA multi-core model, this phenomenon was assessed on both the iPhone 13 and iPhone 14 Pro multi-core models as part of the transfer learning process. This evaluation aimed to preserve the performance of the model across different devices without losing accuracy or previously acquired knowledge during transfer learning. This process involved initially testing the accuracy of each device's multi-core model before applying any transfer learning. Following this, the three phases of transfer learning — inductive learning, feature extraction, and fine-tuning — were conducted using a single-core dataset specific to each device. Once the multi-core model of the iPhone 13 and iPhone 14 Pro had been trained on these new data, the accuracy was retested on the original data to assess whether it had retained its initial performance after undergoing transfer learning. This approach helps to verify that the model remains reliable and does not suffer from catastrophic forgetting after learning new data.

To effectively address catastrophic forgetting and accurately report variations in accuracy, the percentage change between different training phases (e.g., before and after transfer learning) is calculated using Equation 1. This approach ensures a clearer representation of even slight variations in accuracy, providing insight into the model's ability to retain learnt knowledge over successive training phases.

$$\text{Percentage_Change} = \frac{\text{New_Accuracy} - \text{Previous_Accuracy}}{\text{Previous_Accuracy}} \times 100 \quad (1)$$

IV. RESULTS

A. EM-SCA MODEL OF MULTI-CORE DEVICES

This section presents the outcomes of our experiments using combined datasets derived from the core clusters of both the iPhone 13 and iPhone 14 Pro. As detailed in Section III-A4, each device's dataset was integrated with its respective core cluster frequencies. We then applied an individual MLP model to these combined datasets for iPhone 13 and iPhone 14 Pro, as outlined in Section III-A5. The resulting performance metrics are analysed and discussed using confusion matrices and accompanying tables. Confusion matrices are generated based on the classification results for

each software activity, with class indices corresponding to those activities listed in Table 4.

TABLE 4. Label indexing of software applications used for classification with the MLP neural network model.

| Class Index | Class Name |
|-------------|-----------------|
| 0 | calendar-app |
| 1 | camera-photo |
| 2 | camera-video |
| 3 | email-app |
| 4 | gallery-app |
| 5 | home-screen |
| 6 | idle |
| 7 | phone-app |
| 8 | sms-app |
| 9 | web-browser-app |

Figure 7a shows the confusion matrices for the classifier applied individually to the combined dataset of the iPhone 13, while Figure 7b presents the confusion matrix for the iPhone 14 Pro, which achieved accuracies of 99.43% and 99.70%, respectively, on the test data. Additionally, our approach is validated through 5-fold cross-validation on the combined dataset of each device, as presented in Table 5, confirming that the 90:10 split ensures a robust model evaluation. Tables 6 and 7 provide the classification report for the respective iPhone 13 and iPhone 14 Pro models. Other machine learning metrics, such as precision, recall, and F1 score, provide results of either 99% or 100% for each class on both the iPhone 13 and iPhone 14 Pro.

TABLE 5. Cross-validation results for the combined dataset of iPhone 13 and iPhone 14 Pro.

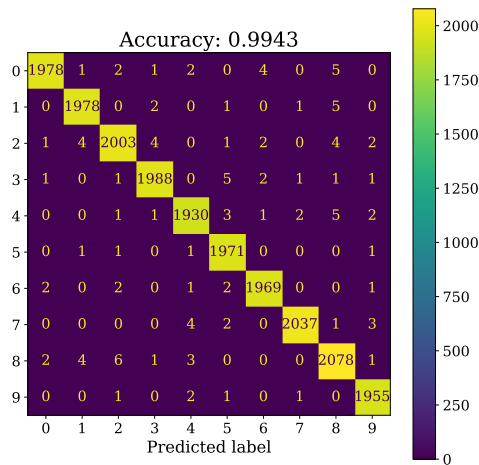
| Combined Dataset | Fold 1 | Fold 2 | Fold 3 | Fold 4 | Fold 5 |
|------------------|--------|--------|--------|--------|--------|
| iPhone 13 | 0.9895 | 0.9943 | 0.9944 | 0.9971 | 0.9960 |
| iPhone 14 Pro | 0.9933 | 0.9947 | 0.9944 | 0.9963 | 0.9953 |

TABLE 6. The classification report of the iPhone 13 combined dataset, assessing 10 software behaviours through a chosen deep learning model.

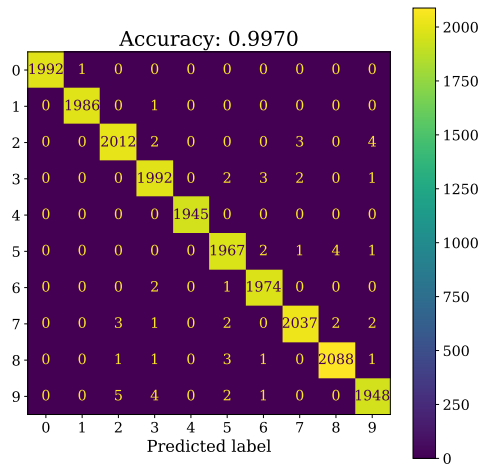
| Class | Precision | Recall | F1-score | Support |
|---------------------|-----------|--------|----------|---------|
| calendar-app (0) | 1.00 | 0.99 | 0.99 | 1993 |
| camera-photo (1) | 0.99 | 1.00 | 1.00 | 1987 |
| camera-video (2) | 0.99 | 0.99 | 0.99 | 2021 |
| email-app (3) | 1.00 | 0.99 | 0.99 | 2000 |
| gallery-app (4) | 0.99 | 0.99 | 0.99 | 1945 |
| home-screen (5) | 0.99 | 1.00 | 1.00 | 1975 |
| idle (6) | 1.00 | 1.00 | 1.00 | 1977 |
| phone-app (7) | 1.00 | 1.00 | 1.00 | 2047 |
| sms-app (8) | 0.99 | 0.99 | 0.99 | 2095 |
| web-browser-app (9) | 0.99 | 1.00 | 1.00 | 1960 |
| Macro Avg | 0.99 | 0.99 | 0.99 | 20000 |
| Weighted Avg | 0.99 | 0.99 | 0.99 | 20000 |
| Accuracy | | | 0.99 | 20000 |

B. COMBINED MODEL ON INDIVIDUAL CORE DATASETS

Two multi-core models were developed, one for the iPhone 13 device and the other for the iPhone 14 Pro device. For each model, the EM data from all CPU cores of the corresponding



(a) iPhone 13



(b) iPhone 14 Pro

FIGURE 7. Confusion matrix for the multi-core dataset from iPhone 13 and iPhone 14 Pro, with labels representing software activities as referenced in Table 4.

TABLE 7. The classification report of the iPhone 14 Pro combined dataset, assessing 10 software behaviours through a chosen deep learning model.

| Class | Precision | Recall | F1-score | Support |
|---------------------|-----------|--------|----------|---------|
| calendar-app (0) | 1.00 | 1.00 | 1.00 | 1993 |
| camera-photo (1) | 1.00 | 1.00 | 1.00 | 1987 |
| camera-video (2) | 1.00 | 1.00 | 1.00 | 2021 |
| email-app (3) | 0.99 | 1.00 | 1.00 | 2000 |
| gallery-app (4) | 1.00 | 1.00 | 1.00 | 1945 |
| home-screen (5) | 0.99 | 1.00 | 1.00 | 1975 |
| idle (6) | 1.00 | 1.00 | 1.00 | 1977 |
| phone-app (7) | 1.00 | 1.00 | 1.00 | 2047 |
| sms-app (8) | 1.00 | 1.00 | 1.00 | 2095 |
| web-browser-app (9) | 1.00 | 0.99 | 0.99 | 1960 |
| Macro Avg | 1.00 | 1.00 | 1.00 | 20000 |
| Weighted Avg | 1.00 | 1.00 | 1.00 | 20000 |
| Accuracy | | | 1.00 | 20000 |

device were used. For the iPhone 13, the accuracy reached 99.94% at a system clock frequency of 3.23 GHz and 99.78% at 1.82 GHz, as shown in Figure 8. The model's performance was higher at the 3.23 GHz core frequency. Similarly, for

the iPhone 14 Pro, the accuracy was 99.91% at 3.46 GHz and 99.99% at 2.02 GHz, with the 2.02 GHz core frequency yielding the best prediction results, as illustrated in Figure 8. Furthermore, the results obtained for the iPhone 13 and iPhone 14 Pro are individually validated through 5-fold cross-validation to ensure the accuracy of the derived outcomes. This shows that regardless of which CPU core's EM emission data is used, the multi-core model does not indicate any significant difference in accuracy.

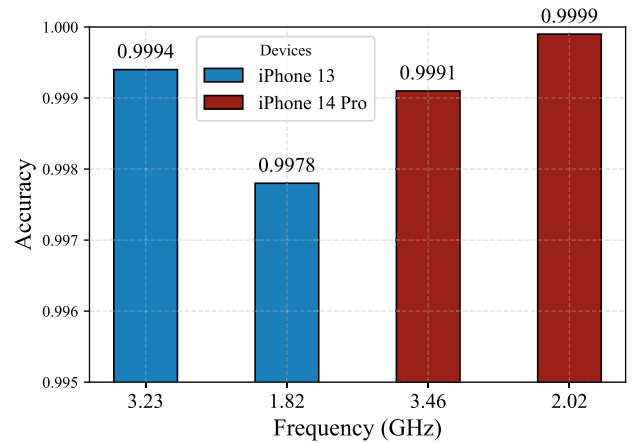


FIGURE 8. Evaluating the accuracy of individual cores of the iPhone 13 and iPhone 14 Pro using the combined dataset from both cores of each device.

C. iPhone 13 MULTI-CORE DEVICE

This section examines the results of applying transfer learning techniques to evaluate the cross-device portability of various datasets from the multi-core iPhone 13 device. Figure 9 presents the accuracy values when applying transfer learning techniques between the combined model of the dedicated cores of the iPhone 13 and the datasets collected at different times, based on the specific system-clock frequency of the core. The x -axis represents the datasets of EM traces captured at different times during the operation of ten different software activities, as described in Section III-A1. Among these, i13-IV- f_1 - t_4 and i13-IV- f_2 - t_4 EM traces were collected simultaneously but at different frequencies, as shown in Figure 4. The y -axis shows the accuracy values for each dataset across three types of transfer learning techniques. The bar plot illustrates the accuracy of each dataset during the transfer learning processes of inductive learning, feature extraction, and fine-tuning.

Both system-clock frequencies yield poor results when applying inductive transfer learning without modifying the multi-core model for new datasets. However, most datasets collected at 3.23 GHz achieve better accuracy, ranging from 60% to 72%, in the feature extraction technique compared to those collected at 1.82 GHz. Despite this, both core-cluster frequencies demonstrate significant improvement, with accuracy reaching approximately 99% during the fine-tuning process.

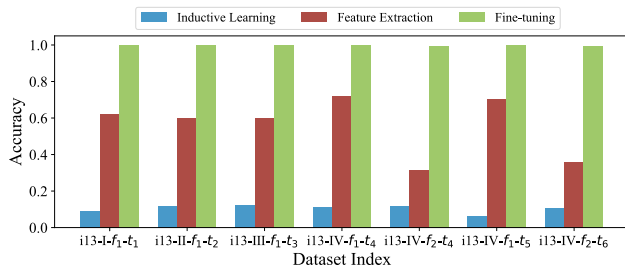


FIGURE 9. Accuracy of three types of transfer learning techniques on datasets collected at different times and frequencies (3.23 GHz and 1.82 GHz) using various iPhone 13 devices.

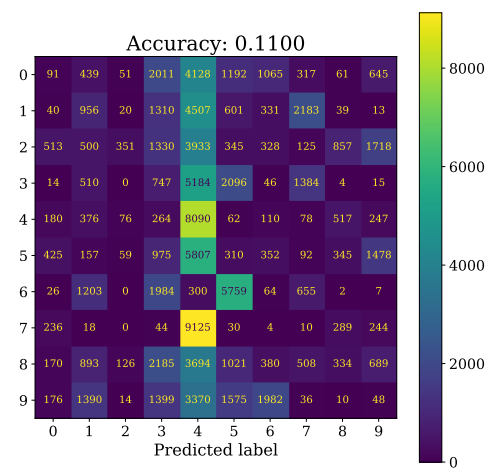
1) EM DATA ACQUISITION FROM iPhone 13 AT 3.23 GHz

Figure 10 presents a comparison of the confusion matrices for three transfer learning techniques: inductive learning, feature extraction, and fine-tuning. These techniques were applied to a newly collected dataset from one of the iPhone 13 devices operating at a system-clock frequency of 3.23 GHz, using a multi-core model of the iPhone 13. The figure highlights how each transfer learning approach impacts classification accuracy and performance, offering a detailed view of the effectiveness of these methods on the dataset. The pattern of the confusion matrices clearly demonstrates how each transfer learning technique aids in classifying the software activities. Among the three techniques, feature extraction provides better predictions, but fine-tuning achieves the most accurate classification across all classes. Figure 11 illustrates the accuracy and loss during the training process when applying the single-core dataset collected at 3.23 GHz from the iPhone 13 to a multi-core model of the iPhone 13, operating at both 3.23 GHz and 1.82 GHz. This comparison uses two transfer learning techniques: feature extraction and fine-tuning. The diagram shows that fine-tuning exhibits a more effective learning pattern, achieving higher accuracy with less loss compared to feature extraction for the given dataset within a much smaller number of epochs.

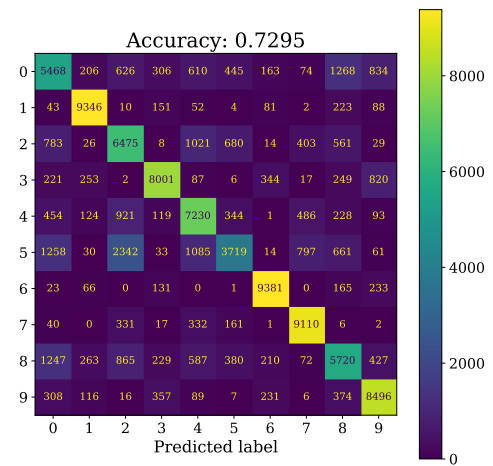
2) EM DATA ACQUISITION FROM iPhone 13 AT 1.82 GHz

Figure 12 presents a comparison of the confusion matrices for the iPhone 13 dataset collected at a frequency of 1.82 GHz with the multi-core models. This dataset was gathered simultaneously with the dataset collected at 3.23 GHz, as described in Section III-A1. The confusion matrix for feature extraction shows lower accuracy and weaker prediction patterns across the classes compared to the dataset collected at the 3.23 GHz system-clock frequency at the same time. However, fine-tuning transfer learning significantly improves the prediction accuracy, reaching approximately 99.6%, which is nearly identical to the accuracy achieved by the other core dataset collected at the same time with fine-tuning. This demonstrates that while feature extraction struggles with accurate classification, fine-tuning consistently delivers high accuracy across both datasets.

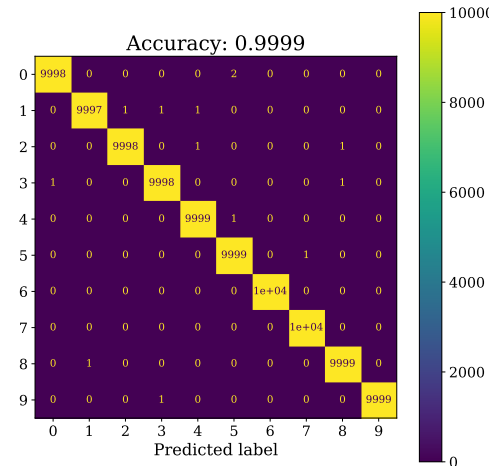
Figure 13 illustrates the learning patterns of both the feature extraction and fine-tuning transfer learning techniques



(a) Inductive Learning



(b) Feature Extraction



(c) Fine-tuning

FIGURE 10. Comparison of the confusion matrix for the i13-IV-f₁-t₄ dataset when applying the three types of transfer learning techniques on the multi-core model of the iPhone 13, with labels referencing Table 4.

applied to the dataset collected from the iPhone 13 at a core frequency of 1.82 GHz at a specific time. The diagram highlights that the fine-tuning technique achieves higher

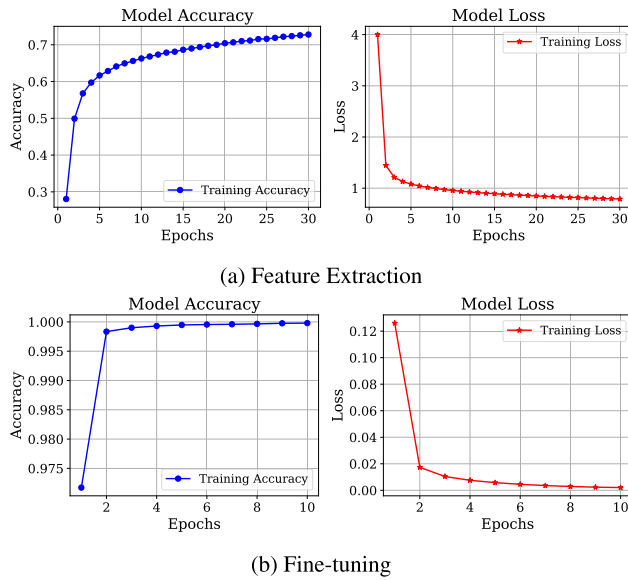


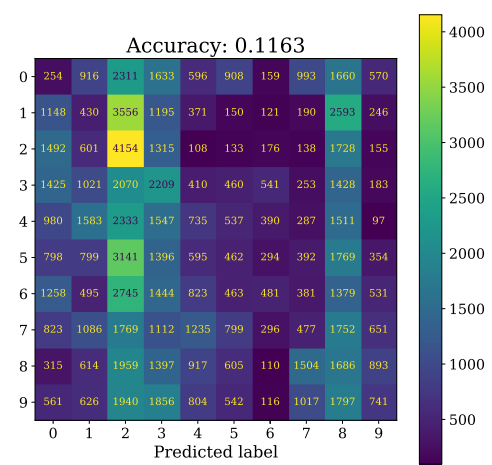
FIGURE 11. The accuracy loss diagram for the feature extraction and fine-tuning processes of the i13-IV- f_1 - t_4 dataset on the multi-core model of the iPhone 13.

accuracy in fewer epochs compared to feature extraction. This demonstrates the efficiency of fine-tuning in rapidly optimising the model, resulting in superior accuracy with reduced training time. In contrast, the feature extraction method requires more epochs to converge, indicating its slower learning curve in this scenario.

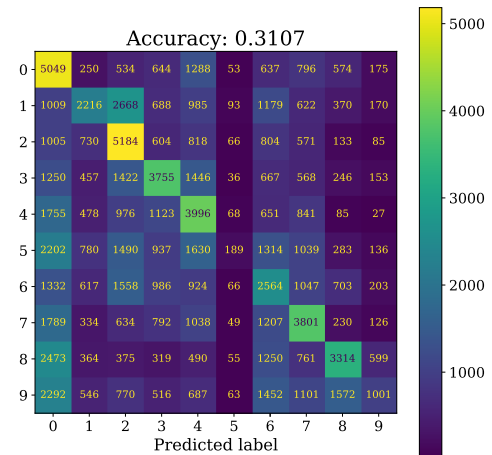
D. iPhone 14 PRO MULTI-CORE DEVICE

This section presents the results of applying transfer learning techniques to assess the cross-device portability of datasets collected from the multi-core iPhone 14 Pro. Figure 14 displays the accuracy of various datasets collected from the iPhone 14 Pro at system-clock frequencies of 3.46 GHz and 2.02 GHz. The two datasets, i14Pro- f_1 - t_7 and i14Pro- f_2 - t_7 , were gathered simultaneously using two HackRF One SDR devices, with each SDR tuned to a specific frequency. The bar graph illustrates the accuracy levels of each dataset across the three stages of the transfer learning process: inductive transfer learning, feature extraction, and fine-tuning, as applied to the iPhone 14 Pro's multi-core model. This comparison highlights the performance of the datasets at each stage, providing insights into the effectiveness of transfer learning techniques at different system-clock frequencies.

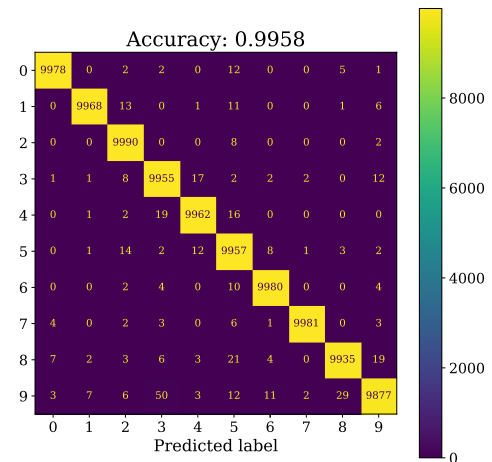
The results reveal varying accuracy transformations at both 3.46 GHz and 2.02 GHz frequencies. Inductive transfer learning demonstrates very poor performance when applied to the multi-core model of the iPhone 14 Pro. In contrast to the iPhone 13, the iPhone 14 Pro achieves better accuracy at 2.02 GHz during the feature extraction stage compared to 3.46 GHz. However, fine-tuning yields excellent accuracy for both system-clock frequencies, with results around 99%. Although 2.02 GHz provides slightly higher accuracy during fine-tuning, the 3.46 GHz frequency also achieves a strong accuracy, close to 99%.



(a) Inductive Learning



(b) Feature Extraction



(c) Fine-tuning

FIGURE 12. Comparison of the confusion matrix for the i13-IV- f_2 - t_4 dataset when applying the three types of transfer learning techniques on the multi-core model of the iPhone 13, with labels referencing Table 4.

1) EM DATA ACQUISITION iPhone 14 PRO AT 3.46 GHz

Figure 15 presents a comparison of the confusion matrices for three transfer learning techniques applied to the

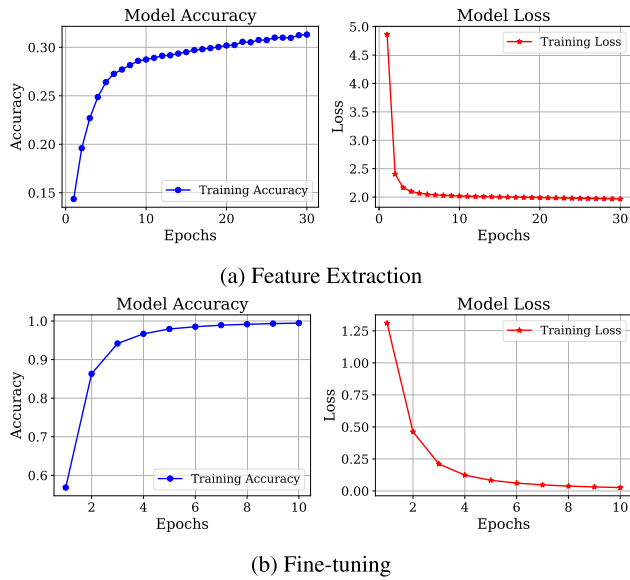


FIGURE 13. The accuracy loss diagram for the feature extraction and fine-tuning processes of the i13-IV- f_2 - t_4 dataset on the multi-core model of the iPhone 13.

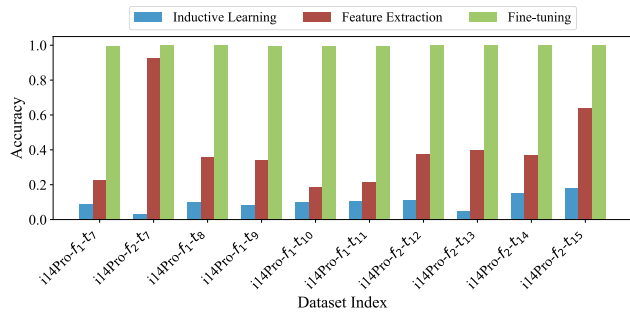
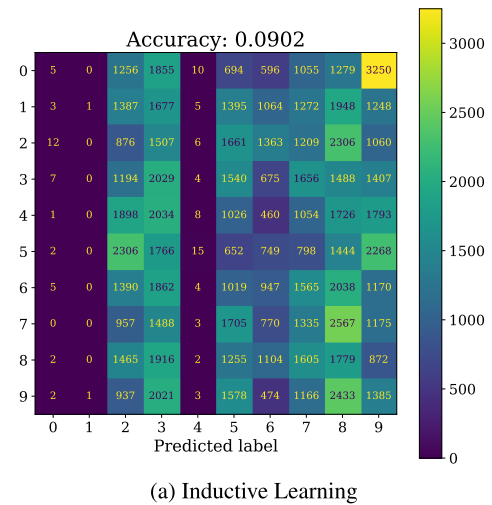
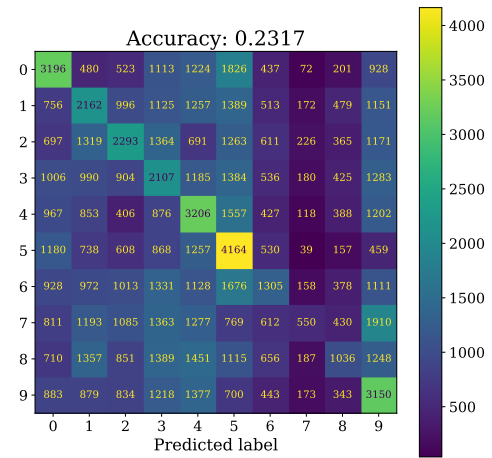


FIGURE 14. Accuracy of three types of transfer learning techniques on datasets collected at different times and frequencies (3.46 GHz and 2.02 GHz) using iPhone 14 Pro smartphone.

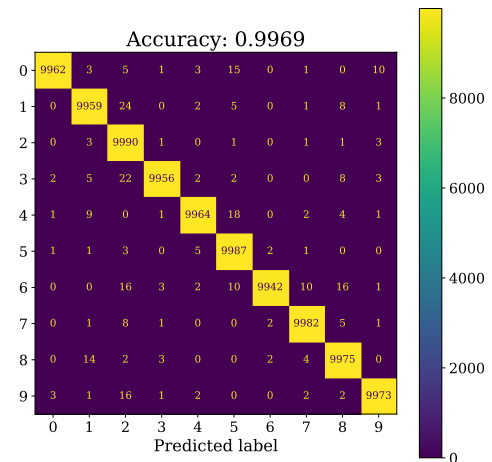
i14Pro- f_1 - t_7 dataset, captured at a system-clock frequency of 3.46 GHz. The prediction performance for various classes using inductive transfer learning and feature extraction techniques falls below expectations, indicating poor classification accuracy. However, accuracy improves significantly when the fine-tuning technique is applied to the multi-core model of the iPhone 14 Pro. Interestingly, these results contrast with those of the iPhone 13, which achieved better performance at a system-clock frequency of 3.23 GHz. This suggests that the iPhone 14 Pro may require different tuning parameters for optimal accuracy compared to the iPhone 13. Additionally, Figure 16 illustrates the learning curve of accuracy and loss when applying feature extraction and fine-tuning techniques to the dataset collected at 3.46 GHz using the multi-core model. The diagram demonstrates that fine-tuning requires fewer epochs to achieve an accuracy of 99%, highlighting its efficiency in optimising the model compared to feature extraction.



(a) Inductive Learning



(b) Feature Extraction



(c) Fine-tuning

FIGURE 15. Comparison of the confusion matrix for the i14Pro- f_1 - t_7 dataset when applying the three types of transfer learning techniques on the multi-core model of the iPhone 14 Pro, with labels referencing Table 4.

2) EM DATA ACQUISITION iPhone 14 PRO AT 2.02 GHz
Unlike the iPhone 13, the iPhone 14 Pro demonstrates better performance at a lower system-clock frequency (2.02 GHz)

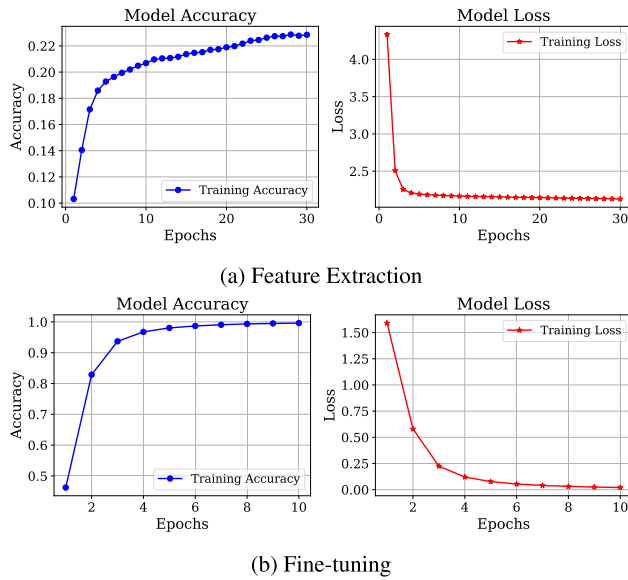


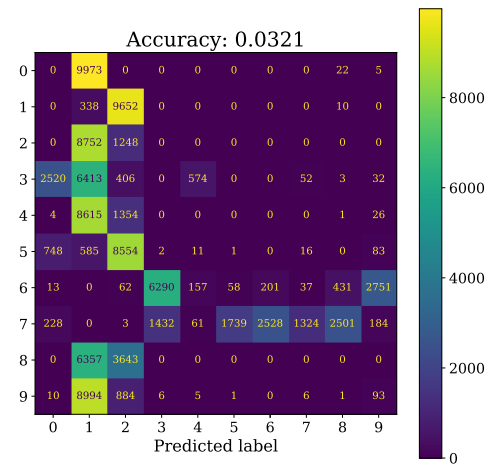
FIGURE 16. The accuracy loss diagram for the feature extraction and fine-tuning processes of the i14Pro- f_1 - t_7 dataset on the multi-core model of the iPhone 14 Pro.

than at the higher frequency of 3.46 GHz. Notably, the i14Pro- f_2 - t_7 dataset achieves significantly higher accuracy during the feature extraction process. Fine-tuning further enhances this performance, improving the classification accuracy for each software activity, as shown in Figure 17. It is important to note that this dataset was collected simultaneously with the i14Pro- f_1 - t_7 dataset, highlighting the distinct behaviour of the two frequencies when applied to transfer learning techniques.

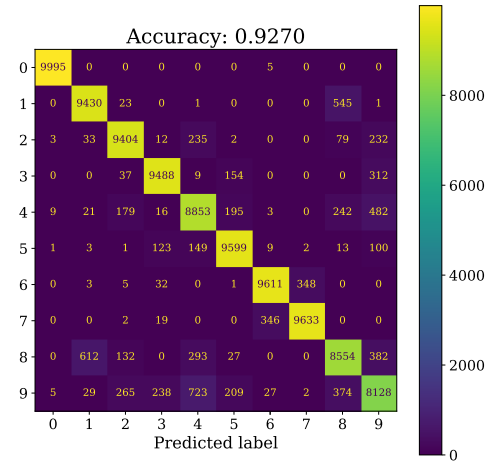
Figure 18 illustrates the learning curves for the feature extraction and fine-tuning transfer learning processes applied to the i14Pro- f_2 - t_7 dataset using the multi-core model of the iPhone 14 Pro. While both learning curves demonstrate high performance, feature extraction takes approximately 25 epochs to reach an accuracy of around 93%. In contrast, the fine-tuning technique achieves 99% accuracy in just 8 epochs. This indicates that, although feature extraction performs well, fine-tuning not only attains a higher accuracy but does so much more quickly, highlighting its efficiency in the learning process.

E. CATASTROPHIC FORGETTING OF MULTICORE MODELS

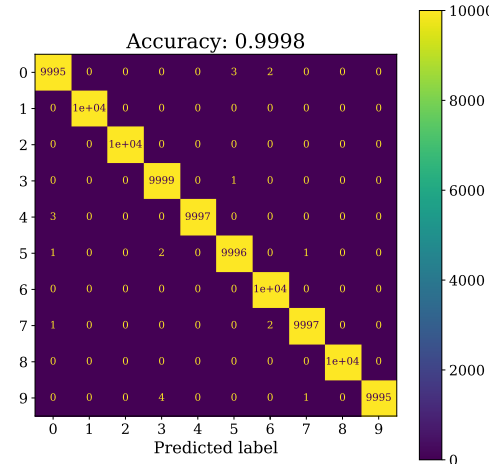
Catastrophic forgetting is a common challenge in transfer learning, where a model forgets previously learnt information when adapting to new tasks. Figure 19 illustrates the confusion matrices of the iPhone 13 and iPhone 14 Pro multi-core models after the transfer learning process, aimed at ensuring the cross-device portability of EM-SCA-based ML models. Previously, Figure 7 presented the confusion matrices of the iPhone 13 and iPhone 14 Pro following the initial training on the combined dataset, before transfer learning. Notably, the accuracy of the confusion matrices remains consistent before and after applying transfer learning, as shown in



(a) Inductive Learning



(b) Feature Extraction



(c) Fine-tuning

FIGURE 17. Comparison of the confusion matrix for the i14Pro- f_2 - t_7 dataset when applying the three types of transfer learning techniques on the multi-core model of the iPhone 14 Pro, with labels referencing Table 4.

Figure 20. This indicates that the models did not experience any significant loss of performance or catastrophic forgetting during the learning process.

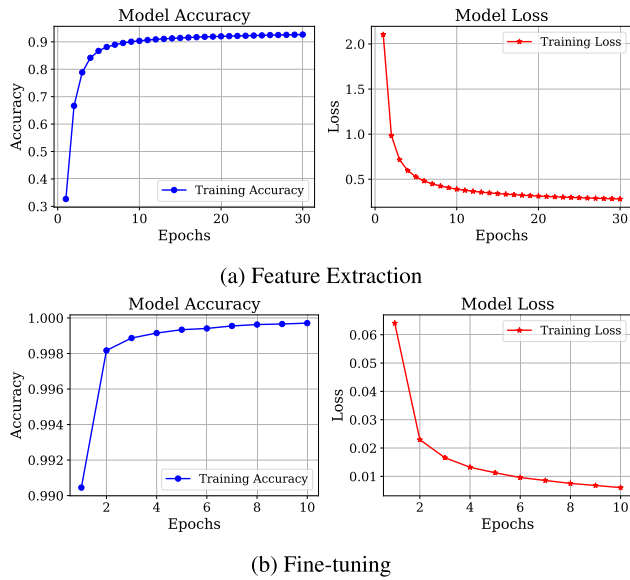


FIGURE 18. The accuracy loss diagram for the feature extraction and fine-tuning processes of the i14Pro- f_2-t_7 dataset on the multi-core model of the iPhone 14 Pro.

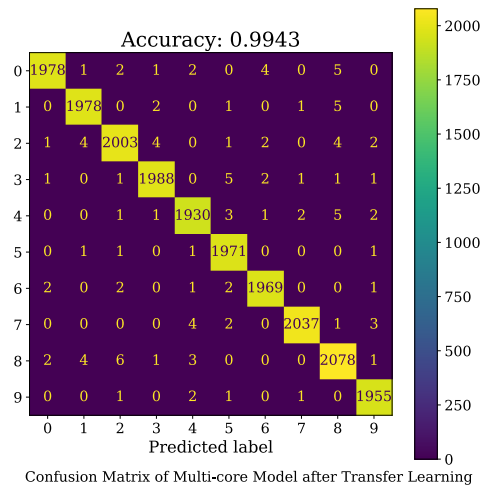
To quantify catastrophic forgetting, we report the percentage change in accuracy across the training phases. The accuracy dropped by 0% when applying transfer learning, highlighting the model's ability to retain previously learnt information. Therefore, it can be concluded that the dedicated transfer learning techniques applied to these models successfully preserved their original accuracy and did not lead to any degradation in classification performance. This comparison helps determine whether the model retains its original classification performance after being exposed to new data through transfer learning.

V. DISCUSSION

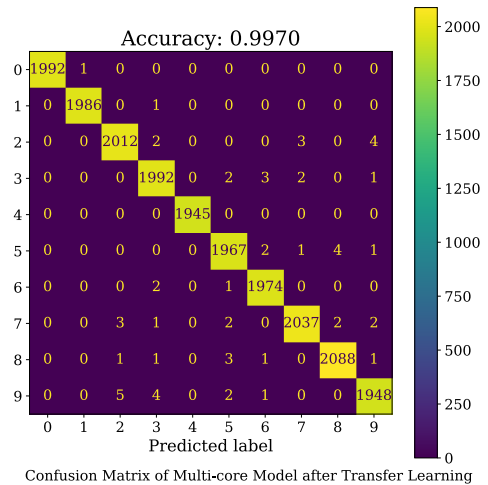
A. FEATURE EXTRACTION OF MULTI-CORE DEVICE

Feature extraction for individual cores in our multi-core model reveals notable differences when implementing cross-device portability, as illustrated in Figures 9 and 14. For the iPhone 13, transfer learning-based cross-device portability achieves higher accuracy at a system-clock frequency of 3.23 GHz compared to 1.82 GHz. In contrast, the iPhone 14 Pro demonstrates significantly higher feature extraction accuracy at the lower frequency of 2.02 GHz relative to its performance at 3.46 GHz.

We hypothesise that this discrepancy—where the iPhone 14 Pro performs better at lower frequencies—arises from several key factors. Specifically, the iPhone 14 Pro benefits from significant architectural improvements brought about by the transition from the A15 Bionic chip to the A16 Bionic chip, which delivers higher instructions per cycle (IPC) and improved efficiency [53]. In addition, advanced power management and thermal design in the A16 Bionic help to mitigate thermal throttling, enabling sustained performance without reliance on higher clock speeds [54].



(a) iPhone 13



(b) iPhone 14 Pro

FIGURE 19. Confusion matrices of iPhone 13 and iPhone 14 Pro multi-core models after the transfer learning process for evaluating catastrophic forgetting, with labels referencing Table 4.

In contrast, the A15 Bionic chip of the iPhone 13 tends to rely more on higher clock speeds for optimal performance, reflecting its earlier design architecture [55]. These enhancements in the iPhone 14 Pro not only improve energy efficiency but also ensure robust performance across a wider range of operating conditions, thereby explaining the observed differences. Our future studies will further explore these variations across diverse scenarios, aiming to uncover the fundamental factors driving the observed performance differences.

B. COMBINED MODEL ON INDIVIDUAL-CORE DATASET

1) iPhone 13

A comparison of datasets acquired at different system-clock frequencies from the two core clusters of the iPhone 13 indicates that the dataset captured at 3.23 GHz yields superior feature extraction accuracy within the multi-core model, outperforming the dataset obtained at 1.82 GHz. While both

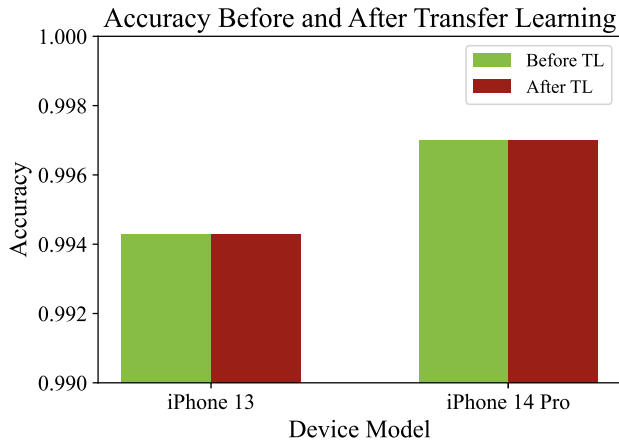


FIGURE 20. Percentage change in accuracy before and after the transfer learning process for iPhone 13 and iPhone 14 Pro, illustrating the impact of catastrophic forgetting.

frequencies yield around 99% accuracy during fine-tuning, the fine-tuning accuracy at 3.23 GHz is consistently higher than that at 1.82 GHz. This suggests that EM traces collected at 3.23 GHz provide more reliable forensic insights compared to those captured at lower core frequencies. Additionally, accuracies achieved through feature extraction and fine-tuning from both core-clusters are further validated using 5-fold cross-validation. Table 8 displays the accuracy obtained in each of the 5 folds, representing the approximate accuracy during feature extraction and fine-tuning for each core-cluster of the iPhone 13. Therefore, investigators can optimise their HackRF One SDR to 3.23 GHz when capturing EM traces from smart devices, enhancing the accuracy of forensic analysis in investigations.

TABLE 8. 5-fold cross-validation of the iPhone 13 dataset across each core-cluster during feature extraction and fine-tuning.

| Fold | iPhone 13 - 3.23 GHz | | iPhone 13 - 1.82 GHz | |
|------|----------------------|-------------|----------------------|-------------|
| | Feature extraction | Fine-tuning | Feature extraction | Fine-tuning |
| 1 | 0.7274 | 0.9931 | 0.3375 | 0.9897 |
| 2 | 0.7101 | 0.9945 | 0.3269 | 0.9936 |
| 3 | 0.7155 | 0.9942 | 0.3904 | 0.9944 |
| 4 | 0.7769 | 0.9947 | 0.3870 | 0.9937 |
| 5 | 0.8017 | 0.9976 | 0.4109 | 0.9943 |

2) iPhone 14 PRO

Fine-tuning transfer learning proves highly effective in detecting software activities across any system-clock frequency of the core-cluster, consistently delivering an accuracy of approximately 99.9%. Although feature extraction can also perform well in certain instances, when considering the integrity and thoroughness required in forensic investigations, fine-tuning emerges as the superior technique. To validate the obtained results, 5-fold cross-validation was performed on both core-cluster datasets during feature extraction and fine-tuning. The results demonstrate consistent

accuracy across each fold, as shown in Table 9. Regardless of the core-cluster's system-clock frequency in smart devices, fine-tuning provides more reliable and accurate results, making it the preferred method for investigating smart devices.

TABLE 9. 5-fold cross-validation of the iPhone 14 Pro dataset across each core-cluster during feature extraction and fine-tuning.

| Fold | iPhone 14 Pro - 3.46 GHz | | iPhone 14 Pro - 2.02 GHz | |
|------|--------------------------|-------------|--------------------------|-------------|
| | Feature extraction | Fine-tuning | Feature extraction | Fine-tuning |
| 1 | 0.2439 | 0.9862 | 0.9593 | 0.9947 |
| 2 | 0.2799 | 0.9945 | 0.9642 | 0.9936 |
| 3 | 0.2735 | 0.9941 | 0.9646 | 0.9945 |
| 4 | 0.3184 | 0.9947 | 0.9661 | 0.9985 |
| 5 | 0.3083 | 0.9946 | 0.9656 | 0.9963 |

C. STUDY LIMITATION

Although we hypothesise that our model is generalisable to multi-core devices, the scope of our study is explicitly limited to two specific iPhone models: iPhone 13 and iPhone 14 Pro. However, we assume that the findings and methodology are applicable to other devices with similar multi-core architectures, particularly within the iPhone series.

VI. CONCLUSION

Dealing with multi-core devices is inevitable in modern digital forensic investigations. Investigating multi-core devices is a critical aspect of forensic insight acquisition, particularly when using a dedicated EM-SCA model. This study explored how different system-clock frequencies of multi-core processors affect the performance of the EM-SCA-based forensic insight acquisition process. To achieve this, this research evaluated the performance of EM-SCA-based ML models on smartphones with multi-core architectures, specifically choosing two devices: the iPhone 13 and iPhone 14 Pro. These smartphones were chosen due to their ability to operate at different clock frequencies based on workload and other parameters.

The EM traces were collected while the devices executed ten different software activities, and a multi-core model was developed by combining the EM data from each core. The multi-core model then underwent a transfer learning process using a separately collected single-core dataset. The evaluation involved three stages of transfer learning techniques: inductive learning, feature extraction, and fine-tuning. The results show that most single-core datasets collected at different times performed poorly during inductive learning. Feature extraction provided intermediate accuracy for each single-core dataset across different frequencies. However, fine-tuning consistently yielded high accuracy—approximately 99%—across all single-core datasets, regardless of the time of collection.

Therefore, it can be concluded that the specific core frequency is not a significant factor when conducting EM-SCA-based forensic insight acquisition on multi-core smart devices specifically the iPhone 13 and iPhone 14 Pro.

Fine-tuning demonstrated superior performance, making it a reliable technique for the cross-device portability of EM-SCA-based ML models. In addition, catastrophic forgetting was tested to assess whether the original model retained its accuracy after the transfer learning process. The results indicated that the accuracy remained stable, confirming that the base model maintained its integrity even after transfer learning.

The performance of the EM-SCA-based ML models in this research has been tested only on two specific smartphones: the iPhone 13 and iPhone 14 Pro. To strengthen the generalisability and robustness of the findings, it is essential to extend this analysis to a broader range of multi-core devices, including various smartphone brands, operating systems, and hardware configurations. This should include not only additional smartphone models from different manufacturers but also IoT devices, which often utilise multi-core architectures. Testing across diverse device types will provide a more comprehensive understanding of the effectiveness of EM-SCA-based forensic insight acquisition. This will ensure its applicability across a wider range of smart technologies while also accounting for various background application behaviours, ultimately refining the methodology and enhancing its robustness.

REFERENCES

- [1] C. Hooper, B. Martini, and K.-K.-R. Choo, "Cloud computing and its implications for cybercrime investigations in Australia," *Comput. Law Secur. Rev.*, vol. 29, no. 2, pp. 152–163, Apr. 2013.
- [2] C. S. D. Brown, "Investigating and prosecuting cyber crime: Forensic dependencies and barriers to justice," *Int. J. Cyber Criminol.*, vol. 9, no. 1, pp. 55–119, Jun. 2015.
- [3] E. Casey, *Digital Evidence and Computer Crime: Forensic Science, Computers, and the Internet*. New York, NY, USA: Academic, 2011.
- [4] B. Nelson, A. Phillips, and C. Steuart, *Guide to Computer Forensics and Investigations*. Boston, MA, USA: Delmar Learning, 2015.
- [5] P. Lutta, M. Sedky, M. Hassan, U. Jayawickrama, and B. B. Bastaki, "The complexity of Internet of Things forensics: A state-of-the-art review," *Forensic Sci. Int., Digit. Invest.*, vol. 38, Sep. 2021, Art. no. 301210.
- [6] H. Arshad, A. B. Jantan, and O. I. Abiodun, "Digital forensics: Review of issues in scientific validation of digital evidence," *J. Inf. Process. Syst.*, vol. 14, no. 2, pp. 346–376, Apr. 2018.
- [7] O. Yakubu, O. Adjei, and N. Babu C., "A review of prospects and challenges of Internet of Things," *Int. J. Comput. Appl.*, vol. 139, no. 10, pp. 33–39, Apr. 2016.
- [8] M. Stoyanova, Y. Nikoloudakis, S. Panagiotakis, E. Pallis, and E. K. Markakis, "A survey on the Internet of Things (IoT) forensics: Challenges, approaches, and open issues," *IEEE Commun. Surveys Tuts.*, vol. 22, no. 2, pp. 1191–1221, 2nd Quart., 2020.
- [9] I. Yaqoob, I. A. T. Hashem, A. Ahmed, S. M. A. Kazmi, and C. S. Hong, "Internet of Things forensics: Recent advances, taxonomy, requirements, and open challenges," *Future Gener. Comput. Syst.*, vol. 92, pp. 265–275, Mar. 2019.
- [10] A. Sayakkara, N.-A. Le-Khac, and M. Scanlon, "Facilitating electromagnetic side-channel analysis for IoT investigation: Evaluating the EMvidence framework," *Forensic Sci. Int., Digit. Invest.*, vol. 33, Jul. 2020, Art. no. 301003.
- [11] A. Sayakkara, N.-A. Le-Khac, and M. Scanlon, "Leveraging electromagnetic side-channel analysis for the investigation of IoT devices," *Digit. Invest.*, vol. 29, pp. S94–S103, Jul. 2019.
- [12] M. R. Zunaidi, A. Sayakkara, and M. Scanlon, "Systematic literature review of EM-SCA attacks on encryption," *arXiv:2402.10030*, 2024.
- [13] A. Sayakkara, N.-A. Le-Khac, and M. Scanlon, "A survey of electromagnetic side-channel attacks and discussion on their case-progressing potential for digital forensics," *Digit. Invest.*, vol. 29, no. 1, pp. 43–54, Jun. 2019.
- [14] A. P. Sayakkara and N.-A. Le-Khac, "Electromagnetic side-channel analysis for IoT forensics: Challenges, framework, and datasets," *IEEE Access*, vol. 9, pp. 113585–113598, 2021.
- [15] A. P. Sayakkara and N.-A. Le-Khac, "Forensic insights from smartphones through electromagnetic side-channel analysis," *IEEE Access*, vol. 9, pp. 13237–13247, 2021.
- [16] L. Navanesan, N.-A. Le-Khac, M. Scanlon, K. De Zoysa, and A. P. Sayakkara, "Ensuring cross-device portability of electromagnetic side-channel analysis for digital forensics," *Forensic Sci. Int., Digit. Invest.*, vol. 48, Mar. 2024, Art. no. 301684.
- [17] L. Navanesan, N.-A. Le-Khac, Y. Oren, K. De Zoysa, and A. P. Sayakkara, "Cross-device portability of machine learning models in electromagnetic side-channel analysis for forensics," *J. Universal Comput. Sci.*, vol. 30, no. 10, pp. 1389–1422, Sep. 2024, doi: 10.3897/jucs.109788.
- [18] A. Zajić and M. Prvulovic, *Understanding Analog Side Channels Using Cryptographic Algorithms*. Cham, Switzerland: Springer, 2023.
- [19] C. Lavaud, R. Gerzaguët, M. Gautier, O. Berder, E. Nogues, and S. Molton, "Whispering devices: A survey on how side-channels lead to compromised information," *J. Hardw. Syst. Secur.*, vol. 5, no. 2, pp. 143–168, Jun. 2021.
- [20] P. Prinetto and G. Roascio, "Hardware security, vulnerabilities, and attacks: A comprehensive taxonomy," in *Proc. ITASEC*, Aug. 2020, pp. 177–189.
- [21] P. C. Kocher, J. Jaffe, and B. Jun, "Differential power analysis," in *Advances in Cryptology—CRYPTO'99*, vol. 1666, Dec. 1999, pp. 388–397.
- [22] D. Agrawal, B. Archambeault, J. R. Rao, and P. Rohatgi, "The EM side—Channel(s)," in *Cryptographic Hardware and Embedded Systems—CHES 2002*. Berlin, Germany: Springer, 2002, pp. 29–45.
- [23] K. Gandolfi, C. Mourtlet, and F. Olivier, "Electromagnetic analysis: Concrete results," in *Cryptographic Hardware and Embedded Systems—CHES 2001*. Berlin, Germany: Springer, May 2001, pp. 251–261.
- [24] S. Picck, G. Perin, L. Mariot, L. Wu, and L. Batina, "SoK: Deep learning-based physical side-channel analysis," *ACM Comput. Surv.*, vol. 55, no. 11, pp. 1–35, Nov. 2023.
- [25] L. Masure, C. Dumas, and E. Prouff, "A comprehensive study of deep learning for side-channel analysis," *IACR Trans. Cryptograph. Hardw. Embedded Syst.*, vol. 2020, pp. 348–375, Nov. 2019.
- [26] B. Hettwer, S. Gehrer, and T. Güneysu, "Applications of machine learning techniques in side-channel attacks: A survey," *J. Cryptograph. Eng.*, vol. 10, no. 2, pp. 135–162, Jun. 2020.
- [27] A. Sayakkara, L. Miralles-Pechuán, N.-A.-L. Khac, and M. Scanlon, "Cutting through the emissions: Feature selection from electromagnetic side-channel data for activity detection," *Forensic Sci. Int., Digit. Invest.*, vol. 32, Apr. 2020, Art. no. 300927.
- [28] G. Hospodar, B. Gierlichs, E. De Mulder, I. Verbauwhede, and J. Vandewalle, "Machine learning in side-channel analysis: A first study," *J. Cryptograph. Eng.*, vol. 1, no. 4, pp. 293–302, Dec. 2011.
- [29] N. Mukhtar, A. P. Fournaris, T. M. Khan, C. Dimopoulos, and Y. Kong, "Improved hybrid approach for side-channel analysis using efficient convolutional neural network and dimensionality reduction," *IEEE Access*, vol. 8, pp. 184298–184311, 2020.
- [30] P. He, Y. Zhang, H. Gan, J. Ma, and H. Zhang, "Side-channel attacks based on attention mechanism and multi-scale convolutional neural network," *Comput. Electr. Eng.*, vol. 119, Oct. 2024, Art. no. 109515.
- [31] A. A. Ahmed, M. K. Hasan, A. Alqahtani, S. Islam, B. Pandey, L. Rzaeva, H. S. Abbas, A. H. M. Aman, and N. Alqahtani, "Deep learning based side-channel attack detection for mobile devices security in 5G networks," *Tsinghua Sci. Technol.*, vol. 30, no. 3, pp. 1012–1026, Jun. 2025.
- [32] A. A. Ahmed and M. K. Hasan, "Design and implementation of side channel attack based on deep learning LSTM," in *Proc. IEEE Region 10 Symp. (TENSYP)*, Sep. 2023, pp. 1–6.
- [33] M. Amar, L. Navanesan, A. P. Sayakkara, and Y. Oren, "Waves of knowledge: A comparative study of electromagnetic and power side-channel monitoring in embedded systems," in *Proc. Int. Conf. Secur. Privacy Cyber-Phys. Syst. Smart Vehicles*. Cham, Switzerland: Springer, 2023, pp. 158–170.

- [34] M. Amar, L. Navanesan, A. Sayakkara, and Y. Oren, "Two's complement: Monitoring software control flow using both power and electromagnetic side channels," in *Proc. 27th Euromicro Conf. Digit. Syst. Design (DSD)*, Aug. 2024, pp. 218–226.
- [35] J. Ai, Z. Wang, X. Zhou, and C. Ou, "Improved wavelet transform for noise reduction in power analysis attacks," in *Proc. IEEE Int. Conf. Signal Image Process. (ICSIP)*, Aug. 2016, pp. 602–606.
- [36] Z. A. Baig, P. Szcwzyk, C. Valli, P. N. Rabadia, P. Hannay, M. Chernyshev, M. N. Johnstone, P. Kerai, A. Ibrahim, K. Sansurooah, N. U. H. Syed, and M. Peacock, "Future challenges for smart cities: Cyber-security and digital forensics," *Digit. Invest.*, vol. 22, pp. 3–13, Sep. 2017.
- [37] A. Ghosh, K. Majumder, and D. De, "A systematic review of digital, cloud and IoT forensics," in *The 'Essence' of Network Security: An End-to-End Panorama*, 2021, pp. 31–74.
- [38] F. Casino, T. Dasaklis, G. Spathoulas, M. Anagnostopoulos, A. Ghosal, I. Borocz, A. Solanas, M. Conti, and C. Patsakis, "Research trends, challenges, and emerging topics in digital forensics: A review of reviews," *IEEE Access*, vol. 10, pp. 25464–25493, 2022.
- [39] A. R. Javed, W. Ahmed, M. Alazab, Z. Jalil, K. Kifayat, and T. R. Gadekallu, "A comprehensive survey on computer forensics: State-of-the-art, tools, techniques, challenges, and future directions," *IEEE Access*, vol. 10, pp. 11065–11089, 2022.
- [40] H. Yu, M. Wang, X. Song, H. Shan, H. Qiu, J. Wang, and K. Yang, "Noise2Clean: Cross-device side-channel traces denoising with unsupervised deep learning," *Electronics*, vol. 12, no. 4, p. 1054, Feb. 2023.
- [41] W. Ahmed, M. Shafique, L. Bauer, and J. H. Karlsruhe, "Adaptive resource management for simultaneous multitasking in mixed-grained reconfigurable multi-core processors," in *Proc. 9th IEEE/ACM/IFIP Int. Conf. Hardw./Softw. Codesign Syst. Synth. (CODES+ISSS)*, Oct. 2011, pp. 365–374.
- [42] J. Noguera and R. M. Badia, "Multitasking on reconfigurable architectures: Microarchitecture support and dynamic scheduling," *ACM Trans. Embedded Comput. Syst.*, vol. 3, no. 2, pp. 385–406, May 2004.
- [43] E. Seo, J. Jeong, S. Park, and J. Lee, "Energy efficient scheduling of real-time tasks on multicore processors," *IEEE Trans. Parallel Distrib. Syst.*, vol. 19, no. 11, pp. 1540–1552, Nov. 2008.
- [44] D. Kim, Y.-B. Ko, and S.-H. Lim, "Energy-efficient real-time multi-core assignment scheme for asymmetric multi-core mobile devices," *IEEE Access*, vol. 8, pp. 117324–117334, 2020.
- [45] M. Ossmann, *Great Scott Gadgets—HackRF One*. Accessed: Oct. 8, 2024. [Online]. Available: <https://greatscottgadgets.com/hackrf/one/>
- [46] A. Pathak, Y. C. Hu, and M. Z. Zhang, "Where is the energy spent inside my app? Fine grained energy accounting on smartphones with eprof," in *Proc. 7th ACM Eur. Conf. Comput. Syst.*, Apr. 2012, pp. 29–42.
- [47] N. Balasubramanian, A. Balasubramanian, and A. Venkataramani, "Energy consumption in mobile phones: A measurement study and implications for network applications," in *Proc. 9th ACM SIGCOMM Conf. Internet Meas.*, Nov. 2009, pp. 280–293.
- [48] X. Chen, A. Jindal, N. Ding, Y. C. Hu, M. Gupta, and R. Vannithamby, "Smartphone background activities in the wild: Origin, energy drain, and optimization," in *Proc. 21st Annu. Int. Conf. Mobile Comput. Netw. (MobiCom)*, vol. 21, Sep. 2015, pp. 40–52.
- [49] J. Danial, D. Das, S. Ghosh, A. Raychowdhury, and S. Sen, "SCNIFFER: Low-cost, automated, efficient electromagnetic side-channel sniffing," *IEEE Access*, vol. 8, pp. 173414–173427, 2020.
- [50] J. Kirkpatrick, R. Pascanu, N. Rabinowitz, J. Veness, G. Desjardins, A. A. Rusu, K. Milan, J. Quan, T. Ramalho, A. Grabska-Barwinska, D. Hassabis, C. Clopath, D. Kumaran, and R. Hadsell, "Overcoming catastrophic forgetting in neural networks," *Proc. Nat. Acad. Sci. USA*, vol. 114, no. 13, pp. 3521–3526, Mar. 2017.
- [51] F. Zenke, B. Poole, and S. Ganguli, "Continual learning through synaptic intelligence," in *Proc. 34th Int. Conf. Mach. Learn.*, vol. 70, Aug. 2017, pp. 3987–3995.

- [52] Z. Li and D. Hoiem, "Learning without forgetting," *IEEE Trans. Pattern Anal. Mach. Intell.*, vol. 40, no. 12, pp. 2935–2947, Dec. 2018.
- [53] Apple Inc. *iPhone*. Accessed: Feb. 19, 2025. [Online]. Available: <https://www.apple.com/iphone/>
- [54] I. Ratkovi, N. Beani, O. S. Nsal, A. Cristal, and V. Milutinovi, "An overview of architecture-level power- and energy-efficient design techniques," *Adv. Comput.*, vol. 98, pp. 1–57, Jan. 2015.
- [55] J. L. Hennessy and D. A. Patterson, *Computer Architecture: A Quantitative Approach*. Amsterdam, The Netherlands: Elsevier, 2011.



include digital forensics, side-channel analysis, and machine learning.



cryptography, digital forensic, ICT4D, and 5G technologies.



His research interests include embedded systems, digital forensics, side-channel analysis, and passive acoustic monitoring. In 2022, he has co-chaired 22nd IEEE Conference on the Advancements of ICT in Emerging Regions (ICTer22) held in Sri Lanka. He serves as a reviewer for various IEEE conferences and journals.

...